

Solventless Surface Photoinitiated Polymerization: Grafting Chemical Vapor Deposition (gCVD)

Tyler P. Martin,^{†‡} Kyra L. Sedransk,^{†‡} Kelvin Chan,[†] Salmaan H. Baxamusa,[†] and Karen K. Gleason^{*,†,‡}

Department of Chemical Engineering and Institute of Soldier Nanotechnology, Massachusetts Institute of Technology, 77 Massachusetts Avenue, Cambridge, Massachusetts 02139-4307

Received January 19, 2007; Revised Manuscript Received March 20, 2007

ABSTRACT: Vapor-phase deposition and characterization of covalently bound polymer coatings using type II surface photoinitiation of the monomers (dimethylamino)methyl styrene (DMAMS) and (diethylamino)ethyl acrylate (DEAEA) are reported. Grafting chemical vapor deposition (gCVD), a solventless, low-temperature process, was first used for coating finished nylon fabric with a previously characterized antimicrobial polymer, PDMAMS. The gCVD process was then further explored using the less-UV-sensitive monomer DEAEA for deposition onto spun-cast PMMA thin films. The structure was confirmed with Fourier transform infrared (FTIR) spectroscopy. Durable films up to 54 nm thick retained 94% of their thickness after 10 rounds of ultrasonication. Optimization of conditions allowed for the deposition of soluble films. Gel permeation chromatography (GPC) and variable-angle spectroscopic ellipsometry (VASE) swelling cell measurements gave an estimated graft density range of 0.06–0.25 chains/nm².

Introduction

Type II photoinitiators are widely used for grafting polymer chains to surfaces.^{1–4} The essential feature of type II initiation involves abstracting a labile hydrogen atom to create a radical. Grafting results when a hydrogen atom is abstracted from a surface and the resulting radical initiates polymerization, leading to a covalently attached polymer chain. The reader is referred to a previous work for a more detailed mechanistic discussion.⁵ Multiple surface-grafted chains result in a polymer film that is chemically bonded to the underlying material. The chemical bonding between the polymer film and the substrate offers many advantages. First, the grafted layer is resistant to abrasion since a covalent bond would have to be broken for a chain to be removed from the surface. Second, the grafted polymer is stable against virtually any solvent, provided that the solvent does not dissolve the underlying layer or cause bond-breaking reactions. This stability allows the surface to be used in solvents that would otherwise dissolve the bulk polymer.

Benzophenone (BP) is a type II initiator that can be excited photochemically with UV irradiation at 254 nm. Grafting using BP has been investigated by a number of researchers.^{1–4} The methods can be divided into three main categories. The most prominent is the all-solution-phase technique: both BP and the monomer are dissolved in a solution in which the surface to be grafted is immersed, or the substrate is sequentially exposed to solutions of each.^{6,7} Alternatively, BP-pretreated surfaces have been exposed to vaporized monomer to effect grafting. This pretreatment can be wet or dry. In the wet case, BP is dissolved in a solution (typically acetone) and cast onto the surface to be grafted. The surface is then dried to remove the solution, leaving behind BP.⁸ The all-dry method exposes the to-be-grafted surface to BP vapor, and the surface uptakes BP during the exposure.^{9–11} Although different, these three categories use the same type II behavior of BP under UV irradiation, resulting in

abstraction of labile hydrogen atoms from the surface to create chain-initiating radicals.

As with thin-film deposition, dry techniques such as chemical vapor deposition (CVD) are becoming increasingly prevalent due to their environmental benefits. The success of all-dry CVD has been demonstrated by methods such as plasma-enhanced CVD (PECVD),^{12–14} hot-filament CVD (HFCVD),^{15–17} and initiated CVD (iCVD).^{18–20} A wide variety of polymeric and organosilicon materials have been made using these methods. CVD is able to produce films of nanoscale thickness with macroscale uniformity on complex geometries.²¹ All-dry processing avoids the wetting and surface-tension effects associated with solution-based coating techniques, so surfaces with nano- or microscale topography can be coated uniformly. The added benefits of grafting motivate the investigation of an iCVD-like grafting process. The envisioned scheme combines the benefits of iCVD and grafting by exposing surfaces to vapors of a type II photoinitiator, BP. All-dry vapor-phase photografting has been demonstrated,^{9–11} but lacks characterization for key features such as molecular weight and graft density. The goal of this work is to use an existing CVD chamber to perform and extensively characterize films produced by solventless grafting, hereby referred to as grafting CVD (gCVD), onto both flat and textile polymer substrates.

Antimicrobial polymer coatings were previously deposited on fabric by initiated CVD (iCVD) from the monomer DMAMS.^{22,23} Grafting CVD (gCVD) is examined to improve the durability of these coatings. However, DMAMS is not an ideal monomer for general optimization of the gCVD process, as it is susceptible to UV irradiation and the deposited polymer is not soluble for gel permeation chromatography (GPC) analysis. It is likely that any of the various vinyl monomers used for iCVD^{18–20,24,25} could be used to deposit grafted layers by gCVD for the creation of desirable surface characteristics. The vinyl monomer DEAEA was chosen for general gCVD optimization because it contains a tertiary amino functional group and so retains some chemical similarity to the functional monomer DMAMS. Also, DEAEA was convenient for two

* Corresponding author. E-mail: kkg@mit.edu.

[†] Department of Chemical Engineering.

[‡] Institute of Soldier Nanotechnology.

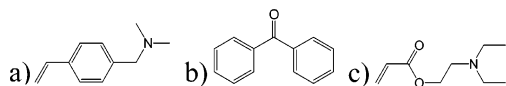


Figure 1. Chemical reactants for grafting CVD: (a) monomer: (dimethylamino)methyl styrene (DMAMS), (b) type II photoinitiator: benzophenone (BP), (c) monomer: (2-diethylamino)ethyl acrylate (DEAEA).

reasons. First, DEAEA experiences negligible degradation under UV exposure, allowing the monomer to retain its structure for subsequent polymerization. Second, DEAEA and its polymer are soluble in water and tetrahydrofuran, facilitating durability characterization, GPC, and swelling. Therefore, molecular weight and graft density of gCVD PDEAEA films can be experimentally determined.

Experimental Section

Depositions were carried out in a custom-built low-pressure reactor (Sharon Vacuum) with a radius of 12 cm and height of 3.3 cm. The top was a quartz plate that allowed laser interferometry and visual inspection of the system. Further details are available.²⁶ A shortwave UV light source (UVG-54, UVP) provided the energy to initiate the reaction. The lamp-to-substrate standoff was 12.5 cm, providing $60 \pm 10 \mu\text{W}/\text{cm}^2$ of 254 nm wavelength irradiation at the growth surface.

The chemical species utilized are shown in Figure 1. The monomer 4-(*N,N*-dimethylamino)methylstyrene (DMAMS), consisting of 50/50 *ortho*- and *para*-isomers (MP-Dajac Laboratories), was vacuum purified before use, vaporized at $346 \pm 2 \text{ K}$, and metered at $2.0 \pm 0.1 \text{ sccm}$ through a mass flow controller (MKS 1153). The monomer 2-(diethylamino)ethyl acrylate (DEAEA) (Aldrich) was vacuum purified before use, vaporized at $351 \pm 2 \text{ K}$, and metered at $1.0 \pm 0.1 \text{ sccm}$ through a mass flow controller (MKS 1153). For gCVD experiments, the initiator benzophenone (BP) (Aldrich) was vacuum purified before use and vaporized at $395 \pm 2 \text{ K}$.

The gCVD process consisted of three phases with the duration of each indicated: initiator application (t_{BP} , 0–60 min), UV pretreatment (t_{UV} , 5–30 min), and UV exposure with monomer flow (t_{M} , 15–60 min, where “M” is either DMAMS or DEAEA). During the first two phases, the pressure was maintained at the system base pressure of 3 mTorr. In the third phase, the monomer pressure was maintained at the specified pressure in the range 75–225 mTorr using a throttling butterfly valve (MKS Instruments 253B). The stage temperature, T_s , was controlled to a specified value within the range 303–318 K using a recirculating chiller/heater (Thermo RTE740). Table 1 lists all sample conditions. All depositions were performed in triplicate.

For deposition of grafted antimicrobial polymer coating, gCVD DMAMS, substrate fabric consisted of the nylon shell of the Army poncho liner (#8405-00-889-3683, Tech. Products Mfg. Corp.), which has a dyed woodland camouflage pattern, a basis weight of approximately $5.3 \text{ mg}/\text{cm}^2$, and average fiber diameter of approximately $15\text{--}18 \mu\text{m}$. Squares of this fabric, $4 \text{ cm} \times 4 \text{ cm}$, were weighed (Mettler Toledo XS205) pre- and post-coating to determine the amount of coating added. The monomer was DMAMS, of which iCVD-deposited coatings were previously optimized²² and shown to be antimicrobial.²³ The stage was maintained at 303 K, and the pressure was 75 mTorr. The fabric was coated on each side. For each side, the time of each deposition phase was $t_{\text{BP}} = 40 \text{ min}$, $t_{\text{UV}} = 5 \text{ min}$, and $t_{\text{M}} = 15 \text{ min}$ (denoted S1 in Table 1). Simultaneous deposition on silicon wafers allowed FTIR characterization (sample S2). For comparison, nongrafted iCVD depositions of PDMAMS were performed as previously described.²³ Briefly, DMAMS and *tert*-amylperoxide (TAP) were fed to the reactor at 2.0 and 0.6 sccm, respectively, at 200 mTorr, and a tungsten filament (Goodfellow) resistively heated to 604 K provided the energy to initiate the reaction. Total coating weight was $131 \pm 6 \text{ mg}/\text{cm}^2$ for samples made using both gCVD and iCVD. Durability testing in phosphate-

buffered saline (PBS) was performed by orbital mixing at 200 rpm for 24 h followed by three rounds of ultrasonication for 10 min each.

Both silicon wafers and PMMA (GPC standard, MW = 18 kDa, polydispersity = 1.04, Scientific Polymer Products) films spun-cast to $\sim 25 \text{ nm}$ thickness on silicon wafer were used as substrates for the gCVD DEAEA runs. It is well known that UV-initiated grafting results in some nongrafted homopolymer.^{1–4} Deposited coatings were rinsed in 37% HCl for 10 min to remove nongrafted material, as it was found that a rinse in deionized (DI) water was insufficient to remove all nongrafted material. The acid rinsing results in more extensive protonation of the basic tertiary amino group than occurs in DI water, thereby solubilizing and removing essentially all nongrafted material. Bare silicon wafers provide a nongraftable surface control; all material was removed from these substrates in the rinse step. Four series of samples, denoted as BP1–BP5, M1–M4, P1–P4, and T1–T4, are fully described in Table 1.

A longer UV pretreatment time of $t_{\text{UV}} = 30 \text{ min}$ was subsequently used for swelling and GPC experiments (samples denoted MW in Table 1). This resulted in the BP initiator producing a higher degree of tethering to the spun-cast PMMA layer and thus reducing the amount of free BP available to cause cross-linking of the deposited polymer chains.

Fourier transform infrared spectroscopy (FTIR) was performed on a Nicolet Nexus 870 ESP used in transmission mode with a liquid nitrogen cooled HgCdTe detector. All spectra were baseline corrected and normalized to film thickness as measured by variable-angle spectroscopic ellipsometry (VASE). For structural comparison, PDMAMS commercial polymer was purchased from MP-Dajac. No commercial standard PDEAEA was available, so iCVD and gCVD FTIR spectra are compared to the monomer. Scanning electron microscopy (SEM) was performed on a JEOL JSM-6060. A thin layer of gold was sputtered prior to imaging to avoid charging.

Variable-angle ellipsometric spectroscopy (VASE, M-2000, J. A. Woollam) was employed as a nondestructive manner of determining film thickness, refractive index, and absorbance. A Cauchy–Urbach isotropic model for index of refraction (n) and extinction coefficient (k) was used to fit the ellipsometric angles Δ and Ψ .²⁷ WVASE32 software from J. A. Woollam was used to perform regressions to the ellipsometric data. A liquid cell (J. A. Woollam) was used in conjunction with VASE to swell grafted polymer layers.²⁴ Films were swelled at room temperature in water controlled at pH 7.0 with phosphate buffer. Ellipsometric data were taken at 75 °C before and after swelling and fit to a Cauchy–Urbach model. Data were taken every 15 s until films had attained equilibrium and stopped swelling. Generally, this took less than 1 min.

Grafted films with underlying PMMA layers were dissolved in tetrahydrofuran (THF) for GPC measurements and compared to a calibration using six PMMA GPC standards representing 1800 to 2 kDa. The narrow peak due to the underlying PMMA that was not grafted to deposited polymer was clear at 18 kDa, with another peak clearly visible at shorter elution time due to the higher molecular weight PDEAEA-grafted PMMA. The GPC system consisted of a Waters 1515 isocratic high-performance liquid chromatography (HPLC) pump, a Waters 2414 differential refractive index detector detecting at 880 nm, and two Styragel HR 4 $7.8 \times 300 \text{ mm}$ columns. Poly(methyl methacrylate) (PMMA) standards (Polymer Laboratories) dissolved in THF were used for calibration at 35 °C.

Results and Discussion

First, the ability of grafting CVD to improve the durability of vapor-deposited polymer coatings over nongrafted iCVD coatings was examined. The iCVD PDMAMS coatings applied to 16 cm^2 squares of nylon fabric retained $25 \pm 3\%$ of their mass (for those starting at $\sim 131 \mu\text{g}/\text{cm}^2$) after the PBS durability test described above. Although iCVD coating is insoluble in

Table 1. Details of gCVD Experimental Runs

sample	monomer	substrate	t_{BP} (min)	t_{UV} (min)	t_M (min)	T_{stage} (K)	P_M (mTorr)	appears in
S1	DMAMS	fabric	40 ^a	5 ^a	15 ^a	303	75	Figure 2
S2	DMAMS	Si wafer	2 × 40 ^b	2 × 5 ^b	2 × 15 ^b	303	75	Figure 3
BP1	DEAEA	PMMA	0	5	15	308	75	Figure 6a
BP2	DEAEA	PMMA	5	5	15	308	75	Figure 6a
BP3	DEAEA	PMMA	15	5	15	308	75	Figure 6a
BP4 ^c	DEAEA	PMMA	30	5	15	308	75	Figure 6a
BP5	DEAEA	PMMA	60	5	15	308	75	Figure 6a
M1 ^c	DEAEA	PMMA	30	5	15	308	75	Figure 6b
M2	DEAEA	PMMA	30	5	30	308	75	Figure 6b
M3	DEAEA	PMMA	30	5	45	308	75	Figure 6b
M4	DEAEA	PMMA	30	5	60	308	75	Figure 6b
P1 ^c	DEAEA	PMMA	30	5	15	308	75	Figure 6c
P2	DEAEA	PMMA	30	5	15	308	125	Figures 4b, 5c, 6c
P3	DEAEA	PMMA	30	5	15	308	175	Figure 6c
P4	DEAEA	PMMA	30	5	15	308	225	Figure 6c
T1	DEAEA	PMMA	30	5	15	303	75	Figure 6d
T2 ^c	DEAEA	PMMA	30	5	15	308	75	Figure 6d
T3	DEAEA	PMMA	30	5	15	313	75	Figure 6d
T4	DEAEA	PMMA	30	5	15	318	75	Figure 6d
MW	DEAEA	PMMA	30	30	15	308	75	Table 2

^a Each side of the fabric substrate is coated with these deposition parameters. ^b The silicon wafer underwent two rounds of deposition on the same side.

^c These four designators denote the same set of three samples at these conditions, but for clarity they are listed under each grouping in which they appear in Figure 6.

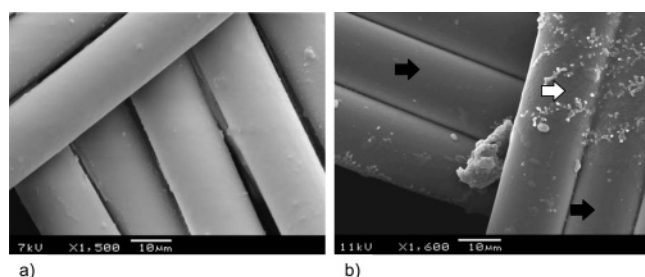


Figure 2. (a) SEM image of gCVD-PDMAMS-coated nylon fibers after severe durability testing. It is clear that the coating remains chiefly intact (sample S1). (b) SEM image of iCVD-PDMAMS-coated nylon fibers after the same durability test. Much of the coating has been removed; cleared areas are marked with a solid arrow, regions where coating remains but is roughened are marked with an open arrow.

PBS, the testing causes the coating to delaminate. By contrast gCVD PDMAMS coatings retained $80 \pm 3\%$ after the same treatment. Indeed, the SEM characterization of gCVD PDMAMS-coated fibers (Figure 2a) shows that the coating remains intact on visible portions of the fibers, whereas much of the coating is lost from the iCVD fibers. It is important to note that iCVD has been previously used to successfully deposit flexible adherent coatings of differing chemistry.^{28,29} It is likely the bulk of the mass loss is from the backsides of fibers and fiber intersections, where the UV irradiation is partially or completely shadow masked. As shown by the FTIR comparison in Figure 3, gCVD PDMAMS has the same major chemical functional groups as the commercial standard and the iCVD film, previously characterized by FTIR.^{22,23} However, there are differences. For instance, the sensitivity of the styrenic monomer at 254 nm resulted in a loss of some of the tertiary-amino functional group, indicated by the marked peaks at 2700–2850 cm^{-1} . The region 1650–1750 cm^{-1} is identified with carbonyl groups formed as atmospheric oxygen combines with untermi-nated radicals upon opening the vacuum chamber, possibly including esters and carboxylic acids for the iCVD spectrum (Figure 3b). The gCVD process (Figure 3c) may also result in amide moieties in the same region, as radicals are not necessarily limited to the carbon backbone. Also, the benzophenone used in gCVD may be represented by peaks at 710 and 1265 cm^{-1} . Due to its UV sensitivity, DMAMS is not well suited for general characterization of the gCVD process, so further work requires

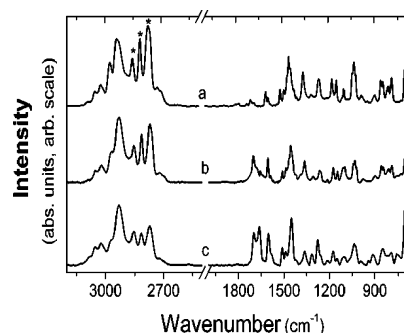


Figure 3. FTIR spectra of (a) commercial standard PDMAMS, (b) iCVD PDMAMS, and (c) gCVD PDMAMS. Peaks attributed to the tertiary amino group at 2700–2850 cm^{-1} are marked (sample S2).

a less UV-sensitive monomer species.

To this end, an acrylate monomer with similar tertiary amino function group, DEAEA, was chosen to perform further exploration of gCVD deposition parameters. Additionally, spun-cast monodisperse PMMA was chosen as the substrate to facilitate further durability and graft density characterization. Initial tests confirmed that grafting did result when the gCVD process employed this monomer. Figure 4 shows the results of durability testing of gCVD and iCVD PDEAEA films in water. In Figure 4a, it is apparent that the water-soluble iCVD polymer is essentially completely removed by just one wash. For the tested samples, consisting of sample P2 in triplicate, an average of 54 ± 13 nm of grafted material remained, and $94 \pm 1\%$ of the film thickness was retained after 10 wash rounds (Figure 4b). Thus the main goal of improving film durability by gCVD is attained.

The chemical structure of the deposited PDEAEA was confirmed by FTIR analysis, shown in Figure 5. The FTIR spectrum of a representative gCVD PDEAEA polymer film (P2, Table 1) is shown with those of the iCVD film and DEAEA monomer. The spectrum of the gCVD film appears noisier than the others due to its relative thinness of 72 nm. The vinyl peaks, denoted by asterisks at 810, 985, 1410, and 1635 cm^{-1} , are present only in the spectrum of the monomer, confirming the vinyl polymerization of DEAEA. Additionally, the peaks assigned to the carbonyl (1735 cm^{-1}) and tertiary amino moieties (2700–2850 cm^{-1}) are present in all the spectra,

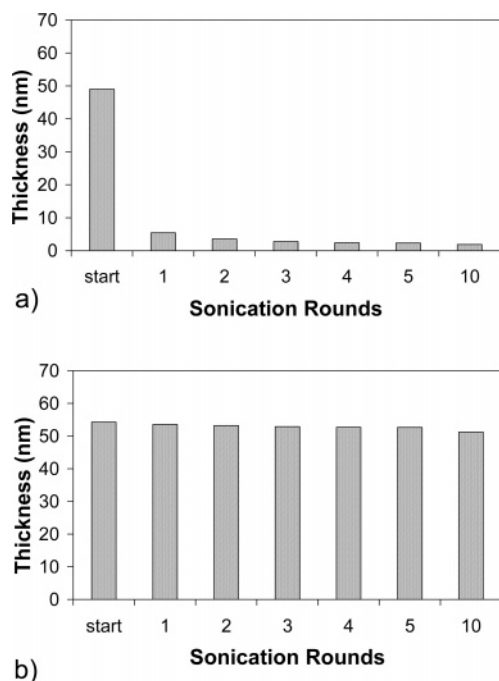


Figure 4. Durability testing of poly(DEAEA) deposited on spun-cast PMMA. (a) Poly(DEAEA) deposited by iCVD, with no grafting or cross-linking; 5% of film is retained after one wash. (b) Poly(DEAEA) deposited by gCVD; 94% of the film is retained after 10 wash rounds (sample P2).

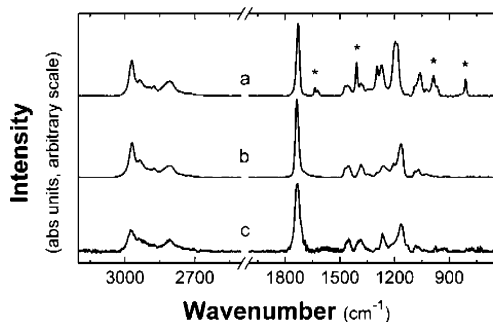


Figure 5. FTIR spectra of the (a) DEAEA monomer, (b) iCVD poly(DEAEA), (c) gCVD poly(DEAEA) (sample P2). The grafted polymer spectrum is consistent with that of the iCVD polymer. Peaks attributed to the vinyl moiety of the monomer are marked with asterisks.

confirming the retention of these pendent groups during the polymerization. Despite the noisiness of the gCVD spectrum, it is clear the spectrum substantially matches that of the iCVD polymer film.

The dependence of grafted thickness on process parameters is shown in Figure 6. First, in Figure 6a, only the duration of the photoinitiator benzophenone (BP) flow is varied (samples BP1–BP5). The control is $t_{BP} = 0$, in which case no growth is expected because of the absence of initiator. However, some film did grow, but the thickness was just 2 nm. The observation of any film formation indicates that the DEAEA monomer reacts with UV radiation alone, but the very thin nature of the deposited layer indicates DEAEA is only slightly sensitive to irradiation at 254 nm. It is expected that the thin film formed has simply been highly cross-linked by the UV radiation and so cannot be washed away. However, film formed in this manner would not be expected to retain any function similar to the linear polymer due to the high degree of cross-linking. Introducing the BP prior to adding the monomer (Figure 6a) results in film thicknesses of 6 nm or greater, confirming that the presence of the type II initiator promotes the deposition process.

Figure 6b shows the results of varying the monomer flow time, t_M . In an ideal vacuum polymerization process, the polymerization would be living and thus the grafted layer thickness would increase linearly with t_M . In this case, however, while an increase in thickness is observed upon increasing t_M from 15 to 30 min, further increases in the duration of the monomer flow period do not increase the grafted layer thickness. The maximum thickness attained by varying monomer flow time is ~ 25 nm. This indicates that the growing chain radicals have all been terminated after 30 min. The growing chains could have terminated through radical combination, disproportionation, or reaction with contaminants in the vacuum chamber.

Monomer partial pressure has been previously shown by our group to be a critical variable in iCVD, a vapor polymerization process.^{30–32} The concentration of monomer at the surface is described by a Burnauer–Emmett–Teller (BET) adsorption isotherm,^{32,33} wherein the surface concentration increases monotonically with the ratio of gas-phase pressures $P_m/P_{m,sat}$, which is the partial pressure of the monomer divided by the monomer's saturation vapor pressure evaluated at the substrate temperature. In this case, the vapor pressure of the monomer is not well known, so the appropriate pressure–substrate temperature combination could not be chosen *a priori*. Figure 6c shows the results of varying the monomer pressure for the gCVD process. This variable is observed to have a much larger affect that the initiator or monomer flow times. An increase in pressure from 75 mTorr to 125 mTorr increased the grafted film thickness from 8 to 54 nm. However, further increasing the pressure is detrimental, as the film formed at 225 mtorr is 34 nm thick after removing nongrafted material. This is likely because the monomer pressure is approaching or is above saturation, and indeed liquid monomer is observed in parts of the reactor, though not on the samples. Such a high concentration of monomer at the surface results in mainly homopolymerization of nongrafted material as the monomer/initiator ratio increases.

A similar trend is observed when the stage temperature is varied. In this case, however, the surface concentration of both monomer and initiator are affected. The result is a wide range of grafted thicknesses, from zero (at 318 K) to 29 nm (at 303 K). Figure 6d shows the plot of this data. Lowering T_s increases the deposited thickness, as would be expected for an absorption-limited process. The discussion above regarding the BET isotherm also applies in this situation. Reducing the T_s decreases $P_{m,sat}$, thereby increasing the monomer concentration at the surface and the coating thickness. Lowering T_s to 298 K resulted in monomer condensation as P_m exceeded $P_{m,sat}$, and so deposition at this T_s is no longer a vapor-phase process but instead a polymerization of the condensed liquid.

Finally, the length of the grafted polymer chains and the density at which they attach to the surface are determined (Table 2, sample MW). The grafted polymer layers were not soluble in THF or other solvents at the short t_{UV} of 5 min, even though they would delaminate from the silicon wafer as the underlying PMMA layer dissolved. However, by increasing t_{UV} to 30 min the entire film, PMMA and grafted layer, was completely soluble when ultrasonicated in THF. The reason for this is twofold: the increased UV time tethers more of the BP to the PMMA layer, and more of the untethered BP is pumped out of the reactor. Both mechanisms reduce the amount of BP available to cause cross-linking. GPC and VASE can be used independently to determine the molecular weight, as

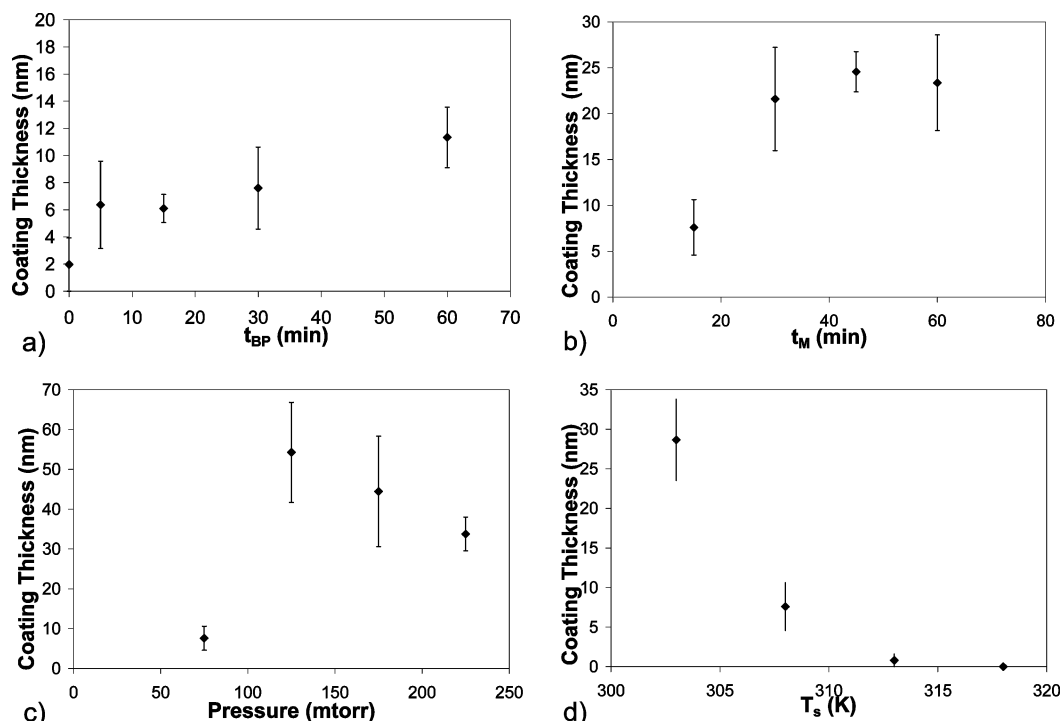


Figure 6. gCVD process optimization. Four deposition variables are explored: (a) initiator time (samples BP1–BP4), (b) monomer time (samples M1–M4), (c) monomer pressure (samples P1–P4), and (d) stage temperature (samples T1–T4).

Table 2. Molecular Weight and Graft Density Found Using GPC and VASE Swelling Cell^a

	GPC	VASE swelling
M_n (kDa)	175 ± 6	72 ± 1
PDI	8–9	
graft density (chain/nm ²)	0.06–0.25	0.24 ± 0.01

^a Hypothetically, GPC provides the maximum MW and minimum graft density, whereas VASE swelling cell data provides the minimum MW and maximum graft density. Thus the two methods bracket the “true” value (sample MW in Table 1).

described by eqs 1 and 2 (from Milner et al.³⁴ and Jordan et al.³⁵).

$$M_{n,\text{GPC}} = M_{n,\text{peak}} - M_{n,\text{PMMA}} \quad (1)$$

$$M_{n,\text{VASE}} = \frac{1.074(h_{\text{swollen}})^{3/2}}{[h_{\text{dry}}(\text{\AA}^2)]^{1/2}} MW_m \quad (2)$$

where $M_{n,\text{GPC}}$ is the grafted chain number average molecular weight determined by GPC, $M_{n,\text{peak}}$ is the number average molecular weight of the early elution time peak, $M_{n,\text{PMMA}}$ is the number average molecular weight of the spun-cast PMMA layer (=18 kDa), $M_{n,\text{VASE}}$ is the grafted chain number average molecular weight determined by VASE with a swelling cell, h_{swollen} is the thickness of the swollen grafted layer in \AA , h_{dry} is the thickness of the dry grafted layer in \AA , and MW_m is the molecular weight of the monomer (=171 for DEAEA). The polymerization method under study may not result solely in linear chains despite the longer UV pretreatment time; some degree of cross-linking may be expected. In this case, GPC will provide the maximum linear chain length, as any branching and/or cross-linking will result in shorter elution times. Conversely, VASE will provide the minimum chain length, as cross-linked chains will swell to a lesser extent. Therefore, the two methods will bracket the “true” value for hypothetical linear chains. The graft density implied by each method is then found using eq 3

(from Feng et al.³⁶), wherein the GPC and VASE techniques will indicate the minimum and maximum graft density, respectively.

$$\sigma = \frac{h_{\text{dry}} \rho N_A}{M_n} \quad (3)$$

where σ is the graft density, ρ is the polymer bulk density (assumed equal to 1 g/mL), N_A is Avogadro’s number, and M_n is the number average molecular weight as determined by GPC or VASE. Table 2 contains the results of characterization by the two methods. There is indeed a spread in values, indicating that some degree of branching/cross-linking is present. Dry films were 28 ± 1 nm and swelled films were 35 ± 1 nm thick. GPC results show a number average molecular weight of 175 kDa with polydispersity (PDI) of 8–9. The relatively high PDI is likely due to the uncontrolled nature of the cross-linking process in this system, resulting in some large chains with many branch points as well as some grafted chains that are relatively short and unbranched. Due to the high PDI, the graft density is estimated in the range 0.06–0.25 chain/nm² from the GPC results. VASE swelling measurements indicate 72 kDa, resulting in a graft density of 0.24 ± 0.01 chain/nm², within the range proscribed by the GPC results. The graft density implied by this range is comparable to that generally achieved by ATRP.^{35,36} According to eq 3, the maximum graft density for this polymer is approximately 0.33 chain/nm², which occurs when the film cannot swell in solvent (i.e., when $h_{\text{swollen}} = h_{\text{dry}}$). Therefore, the graft density achieved by gCVD is near the maximum attainable density. The results show that accurate molecular weight and graft density characterization of UV photografted chains should include both GPC and VASE swelling methods.

Conclusions

Covalently bound polymer coatings have been applied to flat and textile substrates by gCVD, an all-dry technique amenable to polymerization of monomers that lack solubility in desirable

solvents. The method is also low temperature, making it ideal for grafting to fragile polymeric substrates. Durable coatings were applied to fabric by gCVD. Further gCVD parameter exploration was performed to expand the process to the full roster of monomers useful for iCVD. Durable layers up to 54 nm thick were formed in 60 min on flat substrates by gCVD. Molecular weight could be determined by GPC and swelling tests and was found to be in the range 72–175 kDa, indicating some branching and/or cross-linking occurred. From this, the graft density was found to be in the range 0.06–0.25 chain/nm², similar to that generally achieved by other grafting techniques. It is anticipated that gCVD can be extended to create polymers using monomers for which the iCVD method has already been demonstrated. This would result in durable hydrogels and superhydrophobic and functionalizable surfaces. Future work will examine other monomer–substrate systems to better understand the range of applicability of the gCVD process.

References and Notes

- (1) Allen, N. S. *Photopolymerisation and Photoimaging Science and Technology*; Elsevier Applied Science: London, 1989.
- (2) Roffey, C. G. *Photopolymerization of Surface Coatings*; Wiley: New York, 1982.
- (3) Belfield, K.; Crivello, J. V. *Photoinitiated Polymerization*; American Chemical Society: Washington, DC, 2003.
- (4) Fouassier, J.-P. *Photoinitiation, Photopolymerization, and Photocuring: Fundamentals and Applications*; Hanser: Munich, 1995.
- (5) Yang, W. T.; Ranby, B. *Macromolecules* **1996**, *29* (9), 3308–3310.
- (6) Ma, H. M.; Davis, R. H.; Bowman, C. N. *Polymer* **2001**, *42* (20), 8333–8338.
- (7) Ma, H. M.; Davis, R. H.; Bowman, C. N. *Macromolecules* **2000**, *33* (2), 331–335.
- (8) Ogiwara, Y.; Kanda, M.; Takumi, M.; Kubota, H. **1981**, *19* (9), 457–462.
- (9) Howard, G. J.; Kim, S. R.; Peters, R. H. *J. Soc. Dyers Colour.* **1969**, *85*, 468.
- (10) Seiber, R. P.; Needles, H. L. *J. Appl. Polym. Sci.* **1975**, *19* (8), 2187–2206.
- (11) Wirsén, A.; Sun, H.; Albertsson, A. C. *Biomacromolecules* **2005**, *6* (5), 2697–2702.
- (12) Hollahan, J. R.; Bell, A. T. *Techniques and Applications of Plasma Chemistry*; Wiley: New York, 1974.
- (13) Yasuda, H. *Plasma Polymerization*; Academic: Orlando, FL, 1985.
- (14) Inagaki, N. *Plasma Surface Modification and Plasma Polymerization*; Technomic: Lancaster, PA, 1996.
- (15) Lau, K. K. S.; Gleason, K. K. *J. Fluor. Chem.* **2000**, *104* (1), 119–126.
- (16) Pryce Lewis, H. G.; Casserly, T. B.; Gleason, K. K. *J. Electrochem. Soc.* **2001**, *148* (12), F212–F220.
- (17) Loo, L. S.; Gleason, K. K. *Electrochem. Solid State Lett.* **2001**, *4* (11), G81–G84.
- (18) Pryce Lewis, H. G.; Caulfield, J. A.; Gleason, K. K. *Langmuir* **2001**, *17* (24), 7652–7655.
- (19) Murthy, S. K.; Olsen, B. D.; Gleason, K. K. *Langmuir* **2002**, *18* (16), 6424–6428.
- (20) Mao, Y.; Gleason, K. K. *Langmuir* **2004**, *20* (6), 2484–2488.
- (21) Pierson, H. O. *Handbook of Chemical Vapor Deposition*, 2nd ed.; Noyes Publications: Norwich, NY, 1999.
- (22) Martin, T. P.; Gleason, K. K. *Chem. Vapor Depos.* **2006**, *(12)*, 685–691.
- (23) Martin, T. P.; Kooi, S. E.; Chang, S. H.; Sedransk, K. L.; Gleason, K. K. *Biomaterials* **2007**, *28*, 909–915.
- (24) Chan, K.; Gleason, K. K. *Langmuir* **2005**, *21* (19), 8930–8939.
- (25) Ma, M. L.; Mao, Y.; Gupta, M.; Gleason, K. K.; Rutledge, G. C. *Macromolecules* **2005**, *38* (23), 9742–9748.
- (26) Lau, K. K. S.; Mao, Y.; Lewis, H. G. P.; Murthy, S. K.; Olsen, B. D.; Loo, L. S.; Gleason, K. K. *Thin Solid Films* **2006**, *501* (1–2), 211–215.
- (27) Thompson, H. G.; McGahan, W. A. *Spectroscopic Ellipsometry and Reflectometry: A User's Guide*; Wiley: New York, 1999.
- (28) O'Shaughnessy, W. S.; Gao, M. L.; Gleason, K. K. *Langmuir* **2006**, *22* (16), 7021–7026.
- (29) O'Shaughnessy, W. S.; Murthy, S. K.; Edell, D. J.; Gleason, K. K. *Biomacromolecules* **2007**, in press.
- (30) Chan, K.; Gleason, K. K. *Macromolecules* **2006**, *39* (11), 3890–3894.
- (31) Lau, K. K. S.; Gleason, K. K. *Macromolecules* **2006**, *39* (10), 3688–3694.
- (32) Lau, K. K. S.; Gleason, K. K. *Macromolecules* **2006**, *39* (10), 3695–3703.
- (33) Brunauer, S.; Emmett, P. H.; Teller, E. *J. Am. Chem. Soc.* **1938**, *(60)*, 309–319.
- (34) Milner, S. T.; Witten, T. A.; Cates, M. E. *Macromolecules* **1988**, *21* (8), 2610–2619.
- (35) Jordan, R.; Ulman, A.; Kang, J. F.; Rafailovich, M. H.; Sokolov, J. *J. Am. Chem. Soc.* **1999**, *121* (5), 1016–1022.
- (36) Feng, W.; Chen, R. X.; Brash, J. L.; Zhu, S. P. *Macromol. Rapid Commun.* **2005**, *26* (17), 1383–1388.

MA070150V